Published in final edited form as:
J Med Chem. 2011 July 28; 54(14): 5097–5107. doi:10.1021/jm200330s.

Antitumor Agents 288. Design, Synthesis, SAR, and Biological Studies of Novel Heteroatom-Incorporated Antofine and Cryptopleurine Analogs as Potent and Selective Antitumor Agents

Xiaoming Yang[†], **Qian Shi**[†,*], **Shuenn-Chen Yang**[§], **Chi-Yuan Chen**[§], **Sung-Liang Yu**[Δ,Φ], **Kenneth F. Bastow**[‡], **Susan L. Morris-Natschke**[†], **Pei-Chi Wu**[‡], **Chin-Yu Lai**[⊥], **Tian-Shung Wu**[#], **Shiow-Lin Pan**[⊥], **Che-Ming Teng**[⊥], **Jau-Chen Lin**[§], **Pan-Chyr Yang**[⊥,*,§,Ψ], and **Kuo-Hsiung Lee**[†,#,*]

[†] Natural Products Research Laboratories, University of North Carolina, Chapel Hill, NC 27599-7568, USA

[‡] Division of Medicinal Chemistry and Natural Products, Eshelman School of Pharmacy, University of North Carolina, Chapel Hill, NC 27599-7568, USA

[§] Institute of Biomedical Sciences, Academia Sinica, Taipei, Taiwan

[Δ] Department of Clinical Laboratory Sciences and Medical Biotechnology, National Taiwan University, Taipei, Taiwan

[⊥] Department of Internal Medicine, College of Medicine, National Taiwan University, Taipei, Taiwan

[Ψ] Division of Genomic Medicine, Research Center for Medical Excellence, National Taiwan University, Taipei, Taiwan

[Φ] Department of Laboratory Medicine, National Taiwan University Hospital, Taipei, Taiwan

[#] Chinese Medicine Research and Development Center, China Medical University and Hospital, Taichung 404, Taiwan

Abstract

Novel heteroatom-incorporated antofine and cryptopleurine analogs were designed, synthesized, and tested against a panel of five cancer cell lines. Two new *S*-13-oxo analogs (**11** and **16**) exhibited potent cell growth inhibition *in vitro* (GI_{50}: 9 nM and 20 nM). Interestingly, both compounds displayed improved selectivity among different cancer cell lines, in contrast to the natural products antofine and cryptopleurine. MOA[a] studies suggested that *R*-antofine promotes dysregulation of DNA replication during early S phase, while no similar effects were observed for **11** and **15** on corresponding replication initiation complexes. Compound **11** also showed greatly reduced cytotoxicity against normal cells and moderate antitumor activity against HT-29 human colorectal adenocarcinoma xenograft in mice without overt toxicity.

[*]To whom correspondence should be addressed. QS. Phone: 919-843-6325. Fax: 919-966-3893. qshi1@email.unc.edu; PCY. Phone: 886-2-2356-2185. Fax: 886-2-2322-4793. pcyang@ntu.edu.tw; KHL. Phone: 919-962-0066. Fax: 919-966-3893. khlee@unc.edu.

Supporting Information Available. Compound data for **3a-l, 7a-q**, and **10a-j**, biological studies, and HPLC analysis of final compounds. This material is available free of charge via the Internet at http://pubs.acs.org.

Introduction

Phenanthroindolizidines and phenanthroquinolizidines, which are natural alkaloids isolated from several plant species such as the *Asclepiadacae* and *Moracae* family,[1] have been investigated intensively in recent years, due to their interesting biological characteristics, including antimicrobial, anti-angiogenic, and anti-inflammatory effects,[2–8] as well as significant cytotoxicity as demonstrated in the NCI 60 cell-line assay (Figure 1).[9] Further studies have shown that these natural products not only exhibit strong inhibitory activity against cancer cell growth, but also significant effects on cancer cells resistant or cross-resistant to many anticancer drugs in the market.[10] Thus, this important class of chemical entities may potentially augment our present arsenal of anticancer drugs. [11, 12]

Although the biological target(s) and MOA of these natural products are currently still unclear, some interesting findings have been reported. A possible mechanism of action might be inhibition of NF-κB signaling, a well-known pathway in the anti-apoptosis and survival of cancer cells, as well as regulation of P-glycoprotein.[13] Other hypotheses, such as inhibition of protein synthesis during chain elongation stage,[14] targeting ribosomal subunits (low-affinity binding pockets have been identified in the 40S, 60S, 70S, and 80S subunits),[15–17] inhibition of hypoxia-inducible factor 1 (HIF-1),[18] inhibition of thymidylate synthase (TS) and dihydrofolate reductase (DHFR),[19–21] suppression of activator protein-1 (AP-1) and cAMP response element (CRE) signaling pathway, and reduction of cell cycle regulatory proteins such as cyclin D_1, cyclin B_1, CDK_1, CDK_2, and CDK_4 *etc*.[10] have also been reported. In addition, evidence has suggested that certain structural analogs might not be functional analogs,[22] and thus, multiple biological targets might exist.

Despite their promise, the potential development of antofine, cryptopleurine, or related natural or synthetic alkaloids as promising drug candidates has been limited, to a large degree, by severe CNS toxicity, such as disorientation and ataxia,[23] and low natural availability. All of these factors combine to justify an urgent need for improving the pharmacokinetic and pharmacodynamic properties, such as polarity, of this compound class through rational structural modifications. However, only limited studies have been reported in this regard, *e.g.*, introduction of a hydroxy group at C14 of phenanthroindolizidines,[24] construction of phenanthrene-based tylophorine analogs,[25–27] and N atom incorporation at C13a of tylophorine,[28] probably due to the lack of a convergent and efficient synthetic methodology. Recently, our group reported a new strategy suitable for producing numerous new phenanthroindolizidine and phenanthroquinolizidine analogs with E-ring modifications.[29] The versatility and significance of this approach lie in the fact that not only does it facilitate the SAR study of E-ring variations, but also, even more importantly, a group of analogs carrying a heterocyclic E-ring or other polar moieties can be generated to potentially overcome CNS toxicity. CNS toxicity is closely associated with the blood-brain barrier (BBB) penetration of a molecule, which is in large part related to its physicochemical properties, such as lipophilicity (cLogP) or polarity, molecular size and charge, polar surface area (PSA), or hydrogen bonding potential, etc., although other factors may also play a role.[30–32] Herein, we report the design, synthesis, *in vitro* anticancer activity, SAR, and mechanistic studies of new antofine and cryptopleurine derivatives with a N or O atom incorporated in the E-ring. The *in vivo* antitumor activity for the most active compound (**11**) is also reported.

Results and discussion

Initially, antofine analogs bearing a N atom at position C12 were designed and synthesized. The key intermediate **1** was prepared via a procedure recently reported by our group. [27] The amino group of **1** (*S* or *R* isomer) was protected initially with a Boc group to give **2**. Then

the hydroxy group was oxidized with Py•SO_3 to an aldehyde, which was then converted to various secondary amines through reductive amination using $NaBH_3CN$. After removal of the Boc group, **3a-3l** were obtained through cyclization with formaldehyde (Scheme 1).

Compounds **3a-3l** were then screened against four cancer cell lines, A549 (lung), DU-145 (prostate), KB (nasopharyngeal), and HCT-8 (colon). The screening results are shown in Table 1. In comparison with *R*-antofine, all 12 compounds exhibited substantially decreased activity with an average GI_{50} over 1 μM. In addition, no cell-line selectivity was observed. Compound **3f** (R = Ph) was the least potent (inactive) with an average GI_{50} value greater than 20 μM. Insertion of a single methylene group between the N and phenyl ring (**3a** and **3j**, R = CH_2Ph) resulted in greater activity (with the *R* isomer approximately two-fold better than the *S* isomer), while addition of a second methylene group (**3d**, R = CH_2CH_2Ph) did not improve activity any further. Generally, the compounds with an aliphatic amino moiety [cyclic (**3g**), straight chain (**3c, 3h,** and **3l**) or branched chain (**3b**)] showed slightly better activity than those bearing an aromatic moiety. Compounds **3h** and **3l** (R = Me) showed the greatest potency among all compounds, and the *R* isomer (**3l**) was slightly more potent than its *S* enantiomer (**3h**). Conversely, **3i** (*S* isomer) was two-fold more active than its *R* isomer (**3k**). These data implied that introduction of a N atom at position C12 of antofine might not improve the cytotoxicity against cancer cell lines, even though it did increase the polarity as predicted by PreADMET.[33]

Next, we studied the effect of N-incorporation in cryptopleurine, both at positions C12 and C13. For the latter compound series, **2** (*S* or *R*) was converted to **4** through oxidation with Py•SO_3 and subsequent reductive amination using glycine methyl ester hydrochloride. The E ring was formed by sequential deprotection with HCl/MeOH and cyclization with Et_3N/MeOH. The resulting intermediate was further protected with a Boc group to give **5** for easy purification. The lactam carbonyl was then reduced to a methylene using BMS/THF to afford **6**. After removal of the Boc group, 13-aza-cryptopleurines (**7a-q**) were obtained through either acylation or reductive amination (Scheme 2).

The GI_{50} values of **7a-q** are listed in Table 2. Although the 13-aza analogs showed significantly reduced activity as compared with *R*-cryptopleurine, some interesting results were observed. Compound **7g,** with a *N*-cyclopropylmethyl substituent, was the most potent analog against the HCT-8 cell line with a GI_{50} value of 0.25 μM, in addition to better selectivity against A549 and HCT-8 versus DU145 and KB. However, **7h**, with a *N*-cyclopropyl substituent, one -CH_2- shorter than **7g**, showed dramatically reduced activity. Similar results were observed from the comparison of **7c** and **7f**, as well as antofine analogs **3f**, **3a**, and **3d**, suggesting that the length of the side chain on nitrogen affects the anticancer activity. It is also interesting to note that **7g** was much more potent than its *R* isomer **7q**, whereas **7m** and **7p** exhibited the reversed order of activity, although to a less significant degree. Of all the tested analogs in this series, compound **7a**, the hydrochloride salt of 13-aza-cryptopleurine, showed considerable anticancer activity against all four tested cell lines, indicating that **7a** might be a promising lead meriting further investigation.

In the following studies, a series of cryptopleurine analogs (**10a-j**) with N replacement at position C12 were synthesized to explore their anticancer activity. Compound **2** was converted to vinylmethyl ether **8** in two steps, oxidation followed by a Wittig reaction using $Ph_3P{=}CH_2OMe$. Compound **8** was then hydrolyzed with $Hg(OAc)_2$ to give aldehyde **9**. The targets, 12-aza-cryptopleurines **10a-j**, were prepared using a similar strategy as described in the synthesis of compounds **3a-l** (Scheme 3).

The GI_{50} values for **10a-j** are listed in Table 3. Overall, the results suggested that N-incorporation at position C12 of cryptopleurine diminished the anticancer activity (lowest

GI_{50} value was 1.12 μM for a 12-aza analog **10j** versus nM values for cryptopleurine). Similar anticancer activity patterns were observed to those described above with the other compound series. Compounds with bulky or aromatic groups, such as a phenyl or benzyl moiety (**10b** or **10d**), exhibited lower activity (> 20 μM), as also observed in the above two series of analogs. Introducing a polar group, such as hydroxyethyl in **10a**/**10i** and *N*,*N*-dimethylamino in **10f**/**10h**, did not lead to increased activity, although some moderate cell-line selectivity was found. The stereochemistry of the analogs also affected the anticancer activity (compare **10a**/**10i**, **10c**/**10g**, and **10f**/**10h**), as was also observed in the above two analog series, although the trends were neither significant nor consistent. Interestingly, in the comparison of **10j** and **7q** (N12 *vs*. N13 substitution), the former compound was significantly more potent than the latter. Likewise, **10g** was more potent than **7o**, likely indicating that the relocation of the N atom could cause a possible conformational change, which led to a differentiation in biological activity.

Even though the above modifications of antofine and cryptopleurine by N incorporation in the E-ring did not provide analogs with enhanced or at least comparable anticancer activity to the natural alkaloids, we extended our studies by investigating the effect of O atom incorporation at corresponding positions. Unfortunately, introduction of the oxygen atom at position C12 of antofine was not successful due to the instability of the resulting analog. However, incorporation of O atom into the E-ring of cryptopleurine at position C12 or C13 was achieved, as described in Scheme 4.

Reaction of **1** with chloroacetyl chloride furnished the intermediate amide, which underwent intramolecular nucleophilic attack using NaH/THF and subsequent reduction using BMS/THF to afford *S*-13-oxo-cryptopleurine **11** and its *R* isomer **12**. For the O replacement at position C12 of cryptopleurine, the aldehyde of **9** was first converted to an hydroxymethyl group by $NaBH_4$ reduction, followed by removal of Boc and subsequent cyclization using HCHO to give *S*-12-oxo-cryptopleurine **13** and its *R* isomer **14** (Scheme 4).

A cytotoxicity evaluation of **11**–**14** against four cancer cell lines was conducted, and the results are summarized in Table 4. It is exciting to note that **11**, with O at position C13, exhibited potent nanomolar anticancer activity with greater selectivity towards the HCT-8 tumor cell line (GI_{50} = 9 nM). In contrast, compound **12**, the *R*-enantiomer of **11,** showed significantly decreased activity. As for the incorporation of O at position C12, both analogs **13** and **14** exhibited much lower potency than *R*-crytopleurine with GI_{50} >1 μM. The slight structural variation among **11**–**14** resulted in significantly different biological activity. Compound **11** might achieve a specific structural conformation that is required for interacting with the target protein leading to the observed anticancer activity. However, further studies are needed to verify such an hypothesis, as the decreased activity of **13** and **14** could also possibly be due to molecular instability (the hemiaminal ether E-ring).

Our study of O incorporation in antofine/cryptopleurine-type compounds was also extended to the previously reported 7-membered E-ring analog **15**.[29] Its O-containing analog **16** was synthesized using similar procedures to those for **11** (Scheme 5). Firstly, the aldehyde of **9** was reduced to a hydroxymethyl group followed by removal of Boc. The resulting amino intermediate was then reacted with chloroacetyl chloride at 0 °C to provide the chloroacetamide, which was subjected to ring closure and subsequent reduction of the amide carbonyl to a methylene with BMS to give compound **16** in 24% yield over five steps.

When tested in parallel for cytotoxicity, both **15** and **16** were more active against A549 and HCT-8 cancer cell lines than against DU145 and KB. Compound **16** was slightly more active than **15** against DU145 and KB cell proliferation, while it was slightly less active against A549 and HCT-8. These results suggested that the remarkable cell-line selectivity of

15 was somewhat decreased by introducing an oxygen atom at C13. Nevertheless, both analogs exhibited strong potency against the HCT-8 cell line, which indicated that phenanthroindolizidine and phenanthroquinolizidine derivatives with a 7-membered E-ring have a new and interesting structural scaffold and could have a great potential for further development as selective anti-colorectal cancer agents.

In consideration of the impressive cytotoxicity, we next aimed our study at the potential mechanism(s) of action of the representative analogs **11** and **15**, as well as *R*-antofine. Our preliminary cDNA microarray data indicated that *R*-antofine had a profound influence on the major replication initiation complexes ORC (origin recognition complex) and MCM (DNA replication licensing factor) in early S phase. The DNA replication licensing factors Cdt1 (DNA replication factor) and CDC6 (cell division control protein 6) were also up-regulated in a dose- or time-dependent manner when CL1-5 cells were exposed to *R*-antofine for 24 and 48 h, as confirmed by RT-PCR (0.01 μg/mL, Figure 2) and Western blot analysis (Figure 3). These data indicated that *R*-antofine promotes dysregulation of DNA replication in lung cancer cells. However, it is not clear whether the cytotoxic effect of *R*-antofine is directly correlated with promoting dysregulation of DNA replication. In general, the effects of **11** and **15** were not significant, falling in between those produced by *R*-antofine and control. An in-depth investigation on diverse cell events should be helpful for further clarification of their mechanism of action. Obviously, the difference in the E-ring structure is involved in these observed effects, and the E-ring is not totally indispensable.

Compound **11** was then selected for an in vivo study in mice against HT-29 human colorectal adenocarcinoma xenograft. Mice in group 1 received vehicle and served as control for all treatment groups. The median time to endpoint (TTE) for mice in the control group was 16.3 days with a range of 13.8–21.9 days. Compound **11**, i.v. at 20 mg/kg (qd to end), produced a median TTE of 21.3 days and caused 1.1% maximum group body weight loss on day 12, indicating statistically significant antitumor activity ($P < 0.05$) and no obvious toxicity. When dosed i.v./i.p. at 20 mg/kg (bid to end), **11** produced a median TTE of 20.9 days and caused 7.2% maximum group body weight loss occurring on day 19. One tumor remained in the study on day 29 and one treatment-related (TR) death occurred on day 20 (Figures 4 and 5). When dosing frequency was increased, no improved efficacy was observed. Interestingly, a similar phenomenon was also reported in previous studies. For instance, the effectiveness of phenanthroindolizidine analogs with C14-OH was found to be highly schedule dependent, *e.g.*, the therapeutic index of DCB-3503 may be lost if given daily instead of every three days.[33] Therefore, a more rationally designed dosing regimen is being investigated in order for the compounds to exert their best tumor inhibitory effects, and meanwhile, reduce toxicity that could result from unnecessary repetitive dosing. Moreover, we tested compound **11** against human umbilical vein endothelial cells (HUVECs, normal cells), and the results indicated that the cytotoxicity of *R*-cryptopleurine was reduced by 30-fold through our modification, as shown in Figure 6 (GI_{50} 320 nM *vs.* 11 nM). Such improved selectivity against cancer cells over normal cells demonstrates that our newly synthesized analogs can potentially reduce unwanted side effects *in vivo*. In summary, compound **11** exhibited potent *in vitro* anticancer activity with improved cell line selectivity and moderate antitumor activity against HT-29 human colorectal adenocarcinoma in male nude-athymic mice at a dose of 20 mg/kg without causing obvious toxicity.

Conclusions

New synthetic antofine and cryptopleurine analogs with varied E-ring size or heteroatom incorporation were designed and prepared. Two analogs, **11** and **16**, were the most active compounds against tested cancer cell lines, with interestingly improved selectivity against HCT-8 cell growth. Mechanistic studies indicated that *R*-antofine is capable of promoting

dysregulation of DNA replication in early S phase, whereas no similar results were found for compounds **11** and **15**. It is still unclear how this activity correlates with the potent cytotoxicity of antofine, and further investigation is ongoing. In our *in vivo* antitumor study, we found that **11** had improved activity on HUVECs and moderate antitumor effect on human HT-29 adenocarcinoma xenograft in mice. However, further studies in other tumor models are warranted to find out which type of tumor affords the most sensitivity and what treatment protocol provides the best therapeutic index. Moreover, compound **16** appears to be an interesting analog that necessitates in-depth investigation, and results will be reported in due course. Additionally, CNS toxicity will also be explored in the future.

Experimental section

All chemicals were used as purchased. Melting points were measured using a Fisher Johns melting apparatus without correction. Proton nuclear magnetic resonance (^{1}H NMR) spectra were measured on a 300 MHz Gemini or a Varian Inova (400 MHz) NMR spectrometer with TMS as the internal standard. The solvent used was $CDCl_3$ unless otherwise indicated. Mass spectra were recorded on a Shimazu-2010 LC/MS/MS instrument equipped with a TurboIonsSpray ion source. All final target compounds were characterized and determined as at least >95% pure by analytical HPLC.

(S)-N-Boc-(6,7,10-trimethoxy-1,2,3,4-tetrahydrodibenzo[*f*,*h*]isoquinolin-3-yl)m ethanol (2)

$(Boc)_2O$ (3.14 g, 14.40 mmol) was added to the amino-alcohol (4.24 g, 12 mmol) in 100 mL of CH_2Cl_2 and Et_3N (6 mL), and the mixture was stirred for 2 h. HCl (50 mL, 1 N) was added and the organic layer was separated, washed with sat. $NaHCO_3$ and brine, and dried over $MgSO_4$. Column chromatography eluting with CH_2Cl_2/MeOH gave 5.20 g of compound **2** as a white solid. Yield: 95.6%; mp 105–107 °C; $[\alpha]^{23}_D$= 85.5 ° (*c* 0.42, $CHCl_3$); ^{1}H NMR (300 MHz, $CDCl_3$): δ 7.89 (s, 2H), 7.81 (d, *J* = 9.0 Hz, 1H), 7.28 (s, 1H), 7.22 (d, *J* = 8.7 Hz, 1H), 5.29 (br s, 1H), 4.84 (m, 1H), 4.61 (br s, 1H), 4.09 (s, 3H), 4.05 (s, 3H), 4.01 (s, 3H), 3.73-3.62 (m, 2H), 3.27 (dd, *J* = 16.5 Hz, *J* = 6.3 Hz, 1H), 3.18 (t, *J* = 16.5 Hz, 1H), 1.55 (s, 9H); ^{13}C NMR (75 MHz, $CDCl_3$): δ 157.9, 156.2, 149.7, 148.8, 130.4, 126.7, 124.0, 123.9, 123.8, 123.4, 122.8, 115.2, 105.1, 104.2, 104.0, 80.6, 62.7, 56.2, 56.0, 55.7, 50.6, 41.0, 28.6 (3×C), 26.5; ESI-HRMS ($[M + H]^+$) calcd for $C_{26}H_{32}NO_6$ 454.2230, found 454.2246.

General procedures for the synthesis of 12*N*-substituted-12-aza-antofine (3a-l)

The aldehyde was obtained using the same procedure as for compound **8**. Various amines were reacted with the aldehyde in MeOH, followed by addition of HOAc and $NaBH_3CN$, which was stirred at r.t. for 4 h. Sat. $NaHCO_3$ was added to quench the reaction and CH_2Cl_2 was used for extraction. The residue was quickly purified through a column and TFA was used to remove the Boc group. Then TFA was removed by evaporation and the residue was dissolved in CH_2Cl_2 (10 mL), to which K_2CO_3 (100 mg) and $MgSO_4$ (0.5 g) were added, followed by HCHO (37%, 0.1 mL). The mixture was stirred at r.t. overnight. Chromatography gave light yellow to white solids. Yield: 40%–80%.

(*S*)-*tert*-Butyl-6,7,10-trimethoxy-3-((2-methoxy-2-oxoethylamino)methyl)-3,4-dih ydrodibenzo[*f*,*h*]isoquinoline-2(1*H*)-carboxylate (4)

The Boc-aldehyde was obtained using the same procedure as compound **8**. Glycine methyl ester hydrochloride (314 mg, 2.5 mmol) and Et_3N (0.35 ml, 2.5 mmol) were added to the aldehyde in MeOH (30 mL), which was stirred for 0.5 h. Then HOAc (0.70 mL, 12 mmol) and $NaBH_3CN$ (165 mg, 2.5 mmol) were added. The mixture was stirred for 2 h until all the aldehyde disappeared. Sat. $NaHCO_3$ was used to quench the reaction and CH_2Cl_2 was used for extraction, and washed with brine, dried over $MgSO_4$. Chromatography gave 635 mg of

compound **4** as a white solid. Yield: 61% over two steps. mp 78–80 °C; $[\alpha]^{23}_{D}$= 91.6 ° (*c* 0.37, $CHCl_3$); ^{1}H NMR (400 MHz, $CDCl_3$): δ 7.92 (s, 1H), 7.91 (d, *J* = 2.4 Hz, 1H), 7.87 (brs, 1H), 7.44-7.42 (m, 2H), 7.29 (s, 1H), 7.25-7.23 (m, 1H), 5.40-5.29 (m, 1H), 4.92-4.78 (m, 1H), 4.56 (m, 1H), 4.11 (s, 3H), 4.05 (s, 3H), 4.02 (s, 3H), 3.66 (s, 3H), 3.47-3.36 (m, 2H), 3.27 (dd, *J* = 16.4 Hz, *J* = 6.4 Hz, 1H), 3.14 (d, *J* = 16.4 Hz, 1H), 2.81 (dd, *J* = 12.0 Hz, *J* = 8.8 Hz, 1H), 2.64 (dd, *J* = 12.0 Hz, *J* = 6.4 Hz, 1H), 1.54 (s, 9H); ESI MS *m*/*z* 525.20 $(M+H)^+$.

(*S*)-13*N*-Boc-11-oxo-13-aza-cryptopleurine (5)

The ester (635 mg, 1.21 mmol) was dissolved in HCl (1.25M in methanol, 15 mL), which was stirred at 50 °C for 1 h. The solvent was removed. 30 mL of MeOH and Et_3N (0.3 mL) were added. The mixture was stirred at r.t. for 2 h. After normal workup, chromatography afforded 404 mg of ring-closed intermediate as a white solid. Using similar procedure as compound **2**, the intermediate was protected by $(Boc)_2O$ to give 456 mg of **5** as a white solid. Yield: 76% over three steps. mp 125–127 °C; $[\alpha]^{23}_{D}$= −202.8 ° (*c* 0.50, $CHCl_3$); ^{1}H NMR (400 MHz, $CDCl_3$): δ 7.89 (s, 1H), 7.88 (d, *J* = 2.8 Hz, 1H), 7.87 (d, *J* = 9.2 Hz, 1H), 7.23 (dd, *J* = 9.2 Hz, *J* = 2.8 Hz, 1H), 7.19 (s, 1H), 5.88 (d, *J* = 17.2 Hz, 1H), 4.49 (d, *J* = 17.2 Hz, 1H), 4.40 (d, *J* = 18.0 Hz, 1H), 4.10 (s, 4H), 4.05 (s, 4H), 4.01 (s, 3H), 3.87-3.77 (m, 2H), 3.16 (m, 2H), 1.51 (s, 9H); ESI MS *m*/*z* 493.10 $(M+H)^+$, 985.20 $(2M+H)^+$.

(*S*)-13*N*-Boc-13-aza-cryptopleurine (6)

To a solution of the amide (456 mg, 0.93 mmol) in THF (30 mL) was added BMS (2M in THF, 2.79 mL), which was stirred at r.t. overnight. 5 mL of MeOH was added and the mixture was refluxed for 1 h. Chromatography afforded 400 mg of **6** as a white solid. Yield: 90%. mp 116–118 °C; $[\alpha]^{23}_{D}$= −182.5 ° (*c* 0.28, $CHCl_3$); ^{1}H NMR (400 MHz, $CDCl_3$): δ 7.88-7.87 (m, 2H), 7.76 (d, *J* = 8.8 Hz, 1H), 7.20 (s, 1H), 7.19 (dd, *J* = 8.8 Hz, *J* = 2.8 Hz, 1H), 4.44 (d, *J* = 15.2 Hz, 1H), 4.29 (m, 1H), 4.11 (m, 1H), 4.09 (s, 3H), 4.05 (s, 3H), 4.00 (s, 3H), 3.66 (d, *J* = 15.2 Hz, 1H), 3.15 (m, 2H), 3.04 (dd, *J* = 16.4 Hz, *J* = 3.2 Hz, 1H), 2.87 (m, 1H), 2.80 (dd, *J* = 16.4 Hz, *J* = 11.8 Hz, 1H), 2.57-2.52 (m, 1H), 2.45 (dt, *J* = 12.0 Hz, 3.2 Hz, 1H); ESI MS *m*/*z* 479.10 $(M+H)^+$.

General procedures for the synthesis of 13*N*-substituted-13-aza-cryptopleurine (7a-q)

(a) 13*N*-Boc-13-aza-cryptopleurine **6** was stirred in HCl/MeOH for 2 h before the solvent was removed *in vacuo*. The solid was collected and washed sequentially with cold MeOH and ether. Then the solid was dissolved in 10 mL of anhydrous CH_2Cl_2 and Et_3N (0.1 mL), to which RCOCl was added at 0 °C. The mixture was stirred at r.t. for 4 h before 1N HCl was added. After routine workup, chromatography afforded from light orange to white solids. Yield: 70% – 80%. (b) Using the same procedures (reductive amination) as compound **4**. Yield: 50% – 80%.

(*S*,*E*/*Z*)-6,7,10-Trimethoxy-3-(2-methoxyvinyl)-1,2,3,4-tetrahydrodibenzo[*f*,*h*]isoq uinoline (8)

N-Boc-alcohol **2** (1.812 g, 4 mmol) was dissolved in CH_2Cl_2 (50 mL) and Et_3N (1.95 mL, 14 mmol) at 0°C, to which Py•SO_3 (2.23 g, 14 mmol) in 10 mL of DMSO was added dropwise. The ice bath was then removed and the mixture was stirred at r.t. until **2** disappeared by TLC. HCl (1N) was added, and the organic layer was then separated and washed with sat. $NaHCO_3$, brine, and dried over $MgSO_4$. In another flask, $Ph_3P^+CH_2OMeCl^-$ (2.74 g, 8 mmol) was added to KO*t*Bu (875 mg, 7.8 mmol) at 0 °C under N_2, which was stirred for 0.5 h. The aldehyde in 20 mL of CH_2Cl_2 was added dropwise, followed by removal of ice bath. The reaction was kept for 2–3 h before sat. NH_4Cl was poured into the mixture. CH_2Cl_2 was used for extraction and the organic layers were washed with sat. $NaHCO_3$ and brine, dried over $MgSO_4$. Chromatography afforded 1.5

g of compound **8** as a light yellow solid. Yield: 78% (*Z*/*E* = 1/2.5) for two steps. mp 150–152 °C; $[\alpha]^{23}_{D}$= 108.1 ° (*c* 0.59, $CHCl_3$); ^{1}H NMR (400 MHz, $CDCl_3$, *E*/*Z* = 2.5:1): δ 7.94-7.91 (m, 2H), 7.88 (d, *J* = 9.2 Hz, 1H), 7.29 (s, 1H), 7.26-7.22 (m, 1H), 6.30 (d, *J* = 12.8 Hz, 0.68H, *E* isomer), 5.86 (dd, *J* = 6.4 Hz, *J* = 1.6 Hz, 0.28 Hz, *Z* isomer), 5.72 (m, 0.31H, *Z* isomer), 5.30-5.25 (d, *J* = 16.8 Hz, 1H+0.67H, *E* isomer), 4.80 (dd, *J* = 12.8 Hz, *J* = 8.4 Hz, 0.71 H, *E* isomer), 4.59 (d, *J* = 17.2 Hz, 1H), 4.42 (dd, *J* = 8.0 Hz, *J* = 6.4 Hz, 0.29H, *Z* isomer), 4.12-4.11 (m, 3H), 4.05-4.04 (m, 3H), 4.03-4.02 (m, 3H), 3.62 (s, 0.71H, *Z* isomer), 3.44-3.32 (m, 1H), 3.36 (s, 2H, *E* isomer), 3.13 (d, *J* = 16.0 Hz, 1H), 1.55 (s, 9H); ESI MS *m*/*z* 480.05 $(M+H)^+$.

(*S*)-2-(6,7,10-Trimethoxy-1,2,3,4-tetrahydrodibenzo[*f*,*h*]isoquinolin-3-yl)acetal dehyde (9)

Compound **8** (1.5 g, 3.12 mmol) was dissolved in THF (50 mL) and H_2O (5mL), to which $Hg(OAc)_2$ (3.0 g, 9.36 mmol) was added at 0 °C. Then the ice bath was removed and the mixture was stirred overnight. Freshly prepared sat. KI (50 ml) was added dropwise at 0 °C for 10 min, and CH_2Cl_2 was used for extraction. The organic layers were collected and washed with brine, dried over $MgSO_4$. Chromatography furnished 1.09 g of compound **9** as light yellow foam. Yield: 75%. mp 98–100 °C; $[\alpha]^{23}_{D}$= 94.4 ° (*c* 0.68, $CHCl_3$); ^{1}H NMR (400 MHz, $CDCl_3$): δ 9.79 (s, 1H), 7.93 (s, 1H), 7.91 (d, *J* = 2.4 Hz, 1H), 7.85 (brs, 1H), 7.26-7.24 (m, 2H), 5.38-5.29 (m, 2H), 4.58 (d, *J* = 16.0 Hz, 1H), 4.11 (s, 3H), 4.05 (s, 3H), 4.02 (s, 3H), 3.38 (dd, *J* = 16.0 Hz, *J* = 6.4 Hz, 1H), 3.12 (d, *J* = 16.4 Hz, 1H), 2.70-2.59 (m, 2H), 1.53 (s, 9H); ESI MS *m*/*z* 466.10 $(M+H)^+$, 488.15 $(M+Na)^+$.

General procedures for the synthesis of 12*N*-substituted-12-aza-cryptopleurine (10a-j)

using similar procedures as compound **3a-l**. Yield: 50% – 70%.

(*S*)-13-Oxa-cryptopleurine (11) and (*R*)-13-Oxa-cryptopleurine (12)

Compound **2** (177 mg, 0.5 mmol) was suspended in dry CH_2Cl_2 (15 mL) and Et_3N (0.14 mL, 1.00 mmol) at 0 °C, to which chloroacetyl chloride (40 μL, 0.50 mmol) in 1 mL of CH_2Cl_2 was added dropwise slowly. The mixture was stirred at 0 °C for 5 h before 1N HCl was added. The organic layer was separated and washed with sat. $NaHCO_3$ and brine, dried over $MgSO_4$. CH_2Cl_2 was removed and the residue was dissolved in anhydrous THF (5 mL), to which NaH (2.1 equiv) was added at r.t. followed by reflux for 2 h. Sat. NH_4Cl was added and CH_2Cl_2 was used for extraction. After workup, the organic layer was dried over $MgSO_4$. Then the residue was dissolved in 10 mL anhydrous THF, BMS (1.50 mL, 6 mmol) was added, which was stirred at r.t. overnight. MeOH (5 mL) was added and the mixture was refluxed for 1 h. Chromatography gave 73 mg of **11** as a white solid. Yield: 38.5% for three steps; white solid; mp 199–201 °C; $[\alpha]^{23}_{D}$= −134.6 ° (*c* 0.52, $CHCl_3$); ^{1}H NMR (300 MHz, $CDCl_3$): δ 7.86-7.85 (m, 2H), 7.74 (d, *J* = 9.0 Hz, 1H), 7.18 (dd, *J* = 9.0 Hz, *J* = 2.4 Hz, 1H), 7.14 (s, 1H), 4.39 (d, *J* = 15.6 Hz, 1H), 4.12 (m, 2H), 4.08 (s, 3H), 4.03 (s, 3H), 4.00 (s, 3H), 3.91-3.83 (m, 1H), 3.66 (d, *J* = 15.6 Hz, 1H), 3.51 (dd, *J* = 11.1 Hz, *J* = 9.0 Hz, 1H), 3.06 (d, *J* = 11.7 Hz, 1H), 2.91-2.87 (m, 1H), 2.76-2.59 (m, 3H); ESI MS *m*/*z* 380.05 $(M+H)^+$. For **12**: mp 196–198 °C; $[\alpha]^{23}_{D}$= 139.6 ° (*c* 0.26, $CHCl_3$); ^{1}H NMR (300 MHz, $CDCl_3$): δ 7.90-7.89 (m, 2H), 7.78 (d, *J* = 9.0 Hz, 1H), 7.20 (dd, *J* = 9.0 Hz, *J* = 2.7 Hz, 1H), 7.20 (s, 1H), 4.44 (d, *J* = 15.6 Hz, 1H), 4.17-4.08 (m, 1H), 4.10 (s, 3H), 4.05 (s, 3H), 4.01 (s, 3H), 4.04-4.00 (m, 1H), 3.92-3.84 (m, 1H), 3.72 (d, *J* = 15.3 Hz, 1H), 3.54 (dd, *J* = 11.1 Hz, *J* = 9.0 Hz, 1H), 3.09 (d, *J* = 11.4 Hz, 1H), 2.98-2.94 (m, 1H), 2.77-2.61 (m, 3H); ^{13}C NMR (75 MHz, $CDCl_3$): δ 157.5, 149.4, 148.4, 130.2, 126.4, 125.1, 124.1, 123.6, 123.4, 123.3, 115.0, 104.7, 103.8, 103.6, 72.3, 67.4, 56.1, 56.0, 55.9, 55.5, 55.1, 54.4, 28.5; ESI MS *m*/*z* 380.05 $(M+H)^+$.

(*S*)-12-Oxa-cryptopleurine (13) and (*R*)-12-Oxa-cryptopleurine (14)

The aldehyde **9** (100 mg, 0.21 mmol) was dissolved in MeOH, to which $NaBH_4$ (19 mg, 0.50 mmol) was added in one portion. The mixture was stirred for 1 h and sat. $NaHCO_3$ was added. After normal workup, 80 mg of white solid was obtained, which was used without further purification. The residue was dissolved in CH_2Cl_2 (10 mL), to which $MgSO_4$, K_2CO_3, and HCHO were added sequentially. The mixture was stirred overnight. After workup, chromatography gave 32 mg of **13** as a white solid. Yield: 40% for two steps; light yellow solid; mp 195–197 °C; $[\alpha]^{23}_D$= −56.8 ° (*c* 0.60, $CHCl_3$); ^{1}H NMR (300 MHz, $CDCl_3$): δ 7.89-7.88 (m, 2H), 7.75 (d, *J* = 9.3 Hz, 1H), 7.22 (s, 1H), 7.19 (dd, *J* = 9.0 Hz, *J* = 2.7 Hz, 1H), 4.79 (d, *J* = 8.4 Hz, 1H), 4.41 (d, *J* = 15.3 Hz, 1H), 4.19 (dd, *J* = 11.1 Hz, *J* = 5.1 Hz, 1H), 4.10 (s, 3H), 4.05 (s, 3H), 4.03 (m, 1H), 4.01 (s, 3H), 3.75-3.65 (m, 2H), 3.17 (dd, *J* = 15.9 Hz, *J* = 3.6 Hz, 1H), 2.95-2.80 (m, 2H), 2.06-1.92 (m, 1H), 1.74 (m, 1H); ESI MS *m*/*z* 380.05 $(M+H)^+$. For **14**: mp 191–192°C; $[\alpha]^{23}_D$= 51.2 ° (*c* 0.60, $CHCl_3$); ^{1}H NMR (300 MHz, $CDCl_3$): δ 7.87-7.86 (m, 2H), 7.73 (d, *J* = 9.0 Hz, 1H), 7.20 (s, 1H), 7.18 (dd, *J* = 9.6 Hz, *J* = 3.0 Hz, 1H), 4.77 (d, *J* = 8.1 Hz, 1H), 4.38 (d, *J* = 15.3 Hz, 1H), 4.18 (dd, *J* = 11.1 Hz, *J* = 4.8 Hz, 1H), 4.09 (s, 3H), 4.04 (s, 3H), 3.99 (s, 3H), 3.98 (d, *J* = 8.1 Hz, 1H), 3.73-3.61 (m, 2H), 3.13 (dd, *J* = 15.9 Hz, *J* = 3.6 Hz, 1H), 2.91-2.72 (m, 2H), 2.02-1.90 (m, 1H), 1.72-1.67 (m, 1H); ^{13}C NMR (75 MHz, $CDCl_3$): δ 157.7, 149.6, 148.5, 130.3, 126.6, 124.7, 124.2, 123.8, 123.7, 123.6, 115.0, 104.9, 104.5, 103.9, 86.5, 68.1, 56.1, 56.0, 55.7, 55.4, 48.0, 33.5, 31.3; ESI MS *m*/*z* 380.05 $(M+H)^+$.

Compound 16

The aldehyde **9** (140 mg, 0.30 mmol) was dissolved in MeOH, to which $NaBH_4$ (76 mg, 2 mmol) was added. The resulting mixture was stirred at r.t. for 1 h before sat. $NaHCO_3$ was added. The mixture was extracted with CH_2Cl_2 and the organic layers were combined, washed with brine, and dried over Na_2SO_4. Then the solvent was removed under reduced pressure and redissolved in TFA/CH_2Cl_2 (1:1, 10 mL), which was stirred for 0.5 h. The mixture was concentrated to remove TFA. The residue was subject to treatment with chloroacetyl chloride and the rest of the synthesis was similar as that of compound **11**. After chromatography, 37 mg of **16** was obtained as a light yellow solid in 24% yield over five steps. mp 183–185 °C; $[\alpha]^{23}_D$= −114.7 ° (*c* 0.19, $CHCl_3$); ^{1}H NMR (400 MHz, $CDCl_3$): δ 7.90 (s, 1H), 7.88 (d, *J* = 2.4 Hz, 1H), 7.75 (d, *J* = 9.2 Hz, 1H), 7.24 (s, 1H), 7.19 (dd, *J* = 9.2 Hz, *J* = 2.4 Hz, 1H), 4.43 (d, *J* = 15.2 Hz, 1H), 4.10 (s, 3H), 4.05 (m, 4H), 4.01 (m, 4H), 3.98-3.90 (m, 3H), 3.20-3.13 (m, 1H), 3.08-3.01 (m, 3H), 2.96-2.91 (m, 1H), 2.25-2.19 (m, 1H), 2.17-2.11 (m, 1H); ^{13}C NMR (100 MHz, $CDCl_3$): δ 157.7, 149.6, 148.6, 130.3, 126.9, 126.6, 125.4, 124.2, 123.9, 123.7, 115.1, 104.9, 104.1, 104.0, 69.9, 66.5, 59.0, 57.6, 57.0, 56.2, 56.1, 55.7, 36.7, 35.5; ESI MS *m*/*z* 394.10 $(M+H)^+$.

Supplementary Material

Refer to Web version on PubMed Central for supplementary material.

Acknowledgments

This study was supported by grant CA17625-32 from the National Cancer Institute awarded to K. H. Lee and grant DOH98-TD-G-111-007 from the National Research Program for Genomic Medicine awarded to P.C. Yang. This study was also supported in part by the Department of Health Cancer Research Center of Excellence (DOH-100-TD-C-111-05).

Abbreviations used

MOA	mechanism of action

NCI	National Cancer Institute
HIF-1	hypoxia-inducible factor 1
TS	thymidylate synthase
DHFR	dihydrofolate reductase
AP-1	activator protein-1
CRE	cAMP response element
CDK	cyclin-dependent kinase
CNS	central neural system
SAR	structure-activity relationship
BBB	blood-brain barrier
PSA	polar surface area
ORC	origin recognition complex
CDC6	cell division control protein 6
RT-PCR	reverse transcription polymerase chain reaction
HUVECs	human umbilical vein endothelial cells

References

1. Gellert E. The indolizidine alkaloids. J Nat Prod. 1982; 45(1):50–73.
2. Xi Z, Zhang R, Yu Z, Ouyang D. The interaction between tylophorine B and TMV RNA. Bioorg Med Chem Lett. 2006; 16(16):4300–4304. [PubMed: 16759858]
3. Wang K, Su B, Wang Z, Wu M, Li Z, Hu Y, Fan Z, Mi N, Wang Q. Synthesis and antiviral activities of phenanthroindolizidine alkaloids and their derivatives. J Agric Food Chem. 58(5): 2703–2709. [PubMed: 20000413]
4. Baumgartner B, Erdelmeier CAJ, Wright AD, Rali T, Sticher O. An antimicrobial alkaloid from *Ficus septica*. Phytochemistry. 1990; 29(10):3327–3330.
5. Bhutani KK, Sharma GL, Ali M. Plant based antiamoebic drugs; Part I. Antiamoebic activity of phenanthroindolizidine alkaloids; common structural determinants of activity with emetine. Planta Med. 1987; 53(6):532–536. [PubMed: 2895482]
6. Banwell MG, Bezos A, Burns C, Kruszelnicki I, Parish CR, Su S, Sydnes MO. C8c-C15 monoseco-analogues of the phenanthroquinolizidine alkaloids julandine and cryptopleurine exhibiting potent anti-angiogenic properties. Bioorg Med Chem Lett. 2006; 16(1):181–185. [PubMed: 16236503]
7. Yang C-W, Chen W-L, Wu P-L, Tseng H-Y, Lee S-J. Anti-inflammatory mechanisms of phenanthroindolizidine alkaloids. Mol Pharmacol. 2006; 69(3):749–758. [PubMed: 16332992]
8. Yang C-W, Chuang T-H, Wu P-L, Huang W-H, Lee S-J. Anti-inflammatory effects of 7-methoxycryptopleurine and structure-activity relations of phenanthroindolizidines and phenanthroquinolizidines. Biochem Biophys Res Commun. 2007; 354(4):942–948. [PubMed: 17274949]
9. NCI 60-cell assay results can be found at http://dtp.nci.nih.gov/dtpstandard/dwindex/index.jsp
10. Gao W, Lam W, Zhong S, Kaczmarek C, Baker David C, Cheng Y-C. Novel mode of action of tylophorine analogs as antitumor compounds. Cancer Res. 2004; 64(2):678–688. [PubMed: 14744785]
11. Li Z, Jin Z, Huang R. Isolation, total synthesis and biological activity of phenanthroindolizidine and phenanthroquinolizidine alkaloids. Synthesis. 2001; (16):2365–2378.
12. Chemler SR. Phenanthroindolizidines and phenanthroquinolizidines: promising alkaloids for anti-cancer therapy. Curr Bioact Compd. 2009; 5(1):2–19. [PubMed: 20160962]

13. Cusack JC Jr, Liu R, Baldwin AS. Jr., Inducible chemoresistance to 7-ethyl-10-[4-(1-piperidino)-1-piperidino]-carbonyloxycamptothe cin (CPT-11) in colorectal cancer cells and a xenograft model is overcome by inhibition of nuclear factor-kappaB activation. Cancer Res. 2000; 60(9):2323–2330. [PubMed: 10811101]
14. Huang MT, Grollman AP. Mode of action of tylocrebrine - effects on protein and nucleic-acid synthesis. Mol Pharmacol. 1972; 8(5):538–550. [PubMed: 4343427]
15. Gupta RS, Siminovitch L. Mutants of CHO cells resistant to the protein synthesis inhibitors, cryptopleurine and tylocrebrine: genetic and biochemical evidence for common site of action of emetine, cryptopleurine, tylocrebrine, and tubulosine. Biochemistry. 1977; 16(14):3209–3214. [PubMed: 560858]
16. Gupta RS, Krepinsky JJ, Siminovitch L. Structural determinants responsible for the biological activity of (−)-emetine, (−)-cryptopleurine, and (−)-tylocrebrine: structure-activity relationship among related compounds. Mol Pharmacol. 1980; 18(1):136–143. [PubMed: 7412757]
17. Dolz H, Vazquez D, Jimenez A. Quantitation of the specific interaction of [14a-3H]cryptopleurine with 80S and 40S ribosomal species from the yeast Saccharomyces cerevisiae. Biochemistry. 1982; 21(13):3181–3187. [PubMed: 7049239]
18. Cai XF, Jin X, Lee D, Yang YT, Lee K, Hong Y-S, Lee J-H, Lee JJ. Phenanthroquinolizidine alkaloids from the roots of *Boehmeria pannosa* potently inhibit hypoxia-inducible factor-1 in AGS human gastric cancer cells. J Nat Prod. 2006; 69(7):1095–1097. [PubMed: 16872154]
19. Rao KN, Bhattacharya RK, Venkatachalam SR. Inhibition of thymidylate synthase and cell growth by the phenanthroindolizidine alkaloids pergularinine and tylophorinidine. Chem Biol Interact. 1997; 106(3):201–212. [PubMed: 9413547]
20. Rao KN, Bhattacharya RK, Veankatachalam SR. Inhibition of thymidylate synthase by pergularinine, tylophorinidine and deoxytubulosine. Indian J Biochem Biophys. 1999; 36(6):442–448. [PubMed: 10844999]
21. Rao KN, Venkatachalam SR. Inhibition of dihydrofolate reductase and cell growth activity by the phenanthroindolizidine alkaloids pergularinine and tylophorinidine: the in vitro cytotoxicity of these plant alkaloids and their potential as antimicrobial and anticancer agents. Toxicol In Vitro. 2000; 14(1):53–59. [PubMed: 10699361]
22. Gao W, Chen AP-C, Leung C-H, Gullen EA, Fuerstner A, Shi Q, Wei L, Lee K-H, Cheng Y-C. Structural analogs of tylophora alkaloids may not be functional analogs. Bioorg Med Chem Lett. 2008; 18(2):704–709. [PubMed: 18077159]
23. Suffness, M.; Douros, J. Anticancer agents based on natural product models. Academic press; p. 465-487.
24. Gao W, Bussom S, Grill SP, Gullen EA, Hu Y-C, Huang X, Zhong S, Kaczmarek C, Gutierrez J, Francis S, Baker DC, Yu S, Cheng Y-C. Structure-activity studies of phenanthroindolizidine alkaloids as potential antitumor agents. Bioorg Med Chem Lett. 2007; 17(15):4338–4342. [PubMed: 17531481]
25. Wei L, Shi Q, Bastow Kenneth F, Brossi A, Morris-Natschke Susan L, Nakagawa-Goto K, Wu T-S, Pan S-L, Teng C-M, Lee K-H. Antitumor agents 253. Design, synthesis, and antitumor evaluation of novel 9-substituted phenanthrene-based tylophorine derivatives as potential anticancer agents. J Med Chem. 2007; 50(15):3674–3680. [PubMed: 17585747]
26. Lin JC, Yang SC, Hong TM, Yu SL, Shi Q, Wei L, Chen HY, Yang PC, Lee KH. Phenanthrene-based tylophorine-1 (PBT-1) inhibits lung cancer cell growth through the Akt and NF-kappaB pathways. J Med Chem. 2009; 52(7):1903–1911. [PubMed: 19284764]
27. Yang X, Shi Q, Liu YN, Zhao G, Bastow KF, Lin JC, Yang SC, Yang PC, Lee KH. Antitumor agents 268. Design, synthesis, and mechanistic studies of new 9-substituted phenanthrene-based tylophorine analogues as potent cytotoxic agents. J Med Chem. 2009; 52(16):5262–5268. [PubMed: 19645447]
28. Wang K, Wang W, Wang Q, Huang R. Efficient synthesis of aza-phenanthroindolizidine and aza-phenanthroquinolizidine and anticancer activities. Lett Org Chem. 2008; 5(5):383–390.
29. Yang XM, Shi Q, Bastow KF, Lee KH. Antitumor Agents. 274. A New Synthetic Strategy for E-Ring SAR Study of Antofine and Cryptopleurine Analogues. Org Lett. 2010; 12(7):1416–1419. [PubMed: 20196574]

30. Alavijeh MS, Chishty M, Qaiser MZ, Palmer AM. Drug metabolism and pharmacokinetics, the blood-brain barrier, and central nervous system drug discovery. NeuroRx. 2005; 2(4):554–571. [PubMed: 16489365]

31. Clark DE. In silico prediction of blood-brain barrier permeation. Drug Discov Today. 2003; 8(20): 927–933. [PubMed: 14554156]

32. van de Waterbeemd H, Camenisch G, Folkers G, Chretien JR, Raevsky OA. Estimation of blood-brain barrier crossing of drugs using molecular size and shape, and H-bonding descriptors. J Drug Target. 1998; 6(2):151–165. [PubMed: 9886238]

33. http://preadmet.bmdrc.org

34. Wang Y, Gao W, Svitkin YV, Chen AP, Cheng YC. DCB-3503, a tylophorine analog, inhibits protein synthesis through a novel mechanism. PLoS One. 5(7):e11607. [PubMed: 20657652]

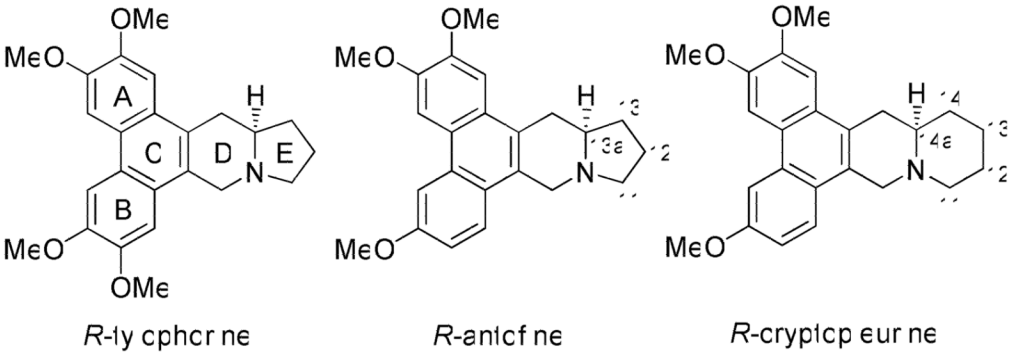

Figure 1.
Representative structures of phenanthroindolizidines and phenanthroquinolizidines

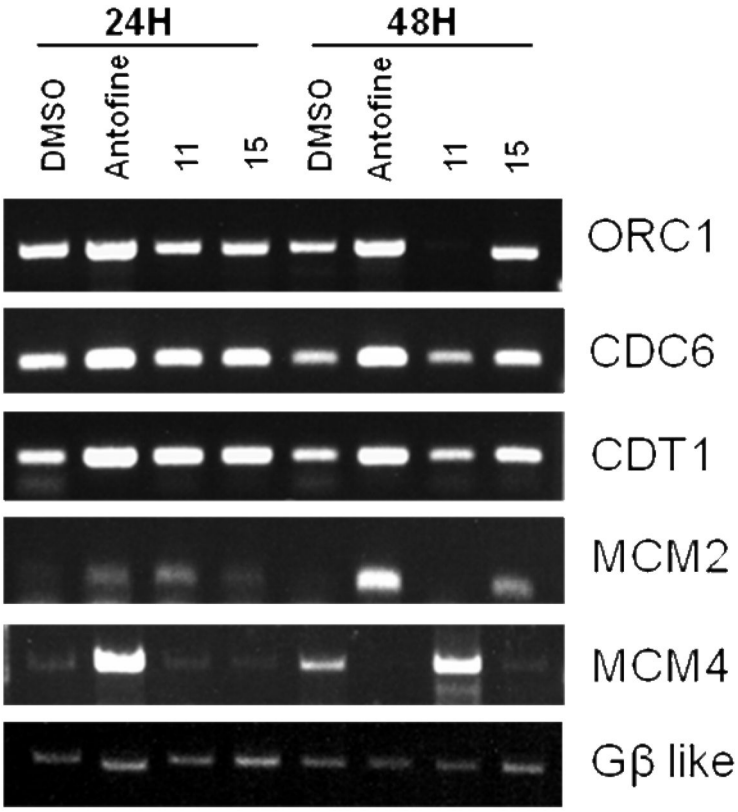

Figure 2.

RT-PCR results of *R*-antofine, **11**, and **15** at 0.01 μg/mL on major DNA replication complexes in CL1-5 cells at 24 and 48 h

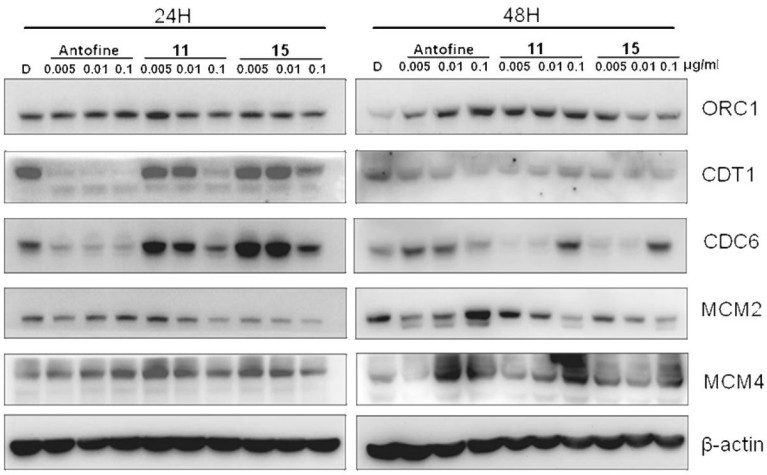

Figure 3.

Western blot analysis of *R*-antofine, **11**, and **15** on major DNA replication complexes in CL1-5 cells at 24 and 48 h

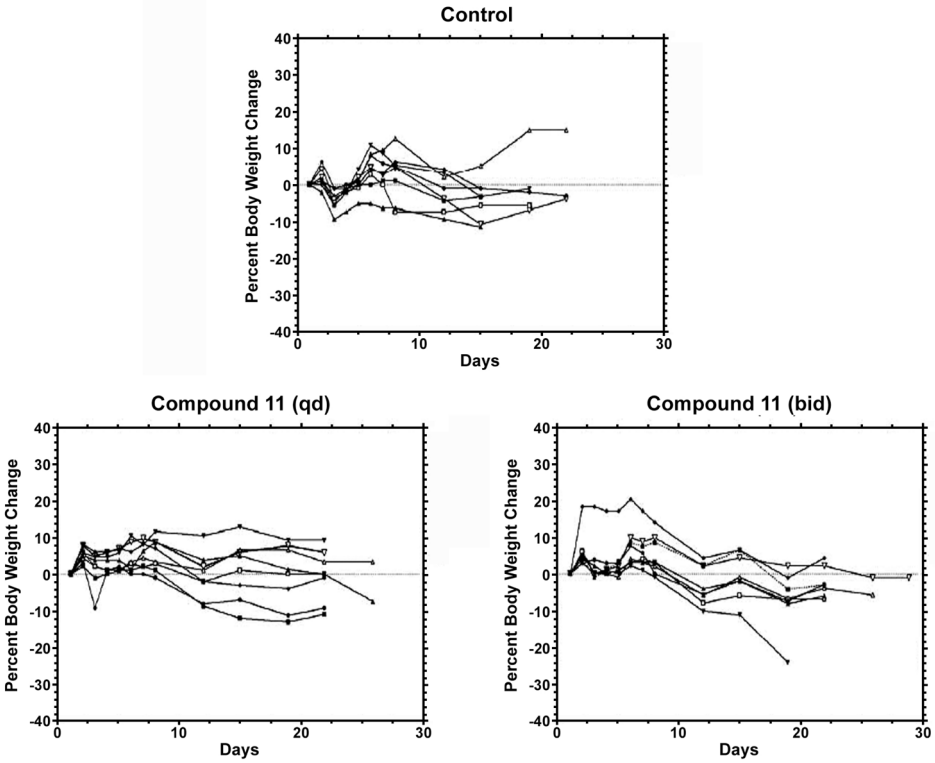

Figure 4.
Individual animal body weight change for control and treatment groups

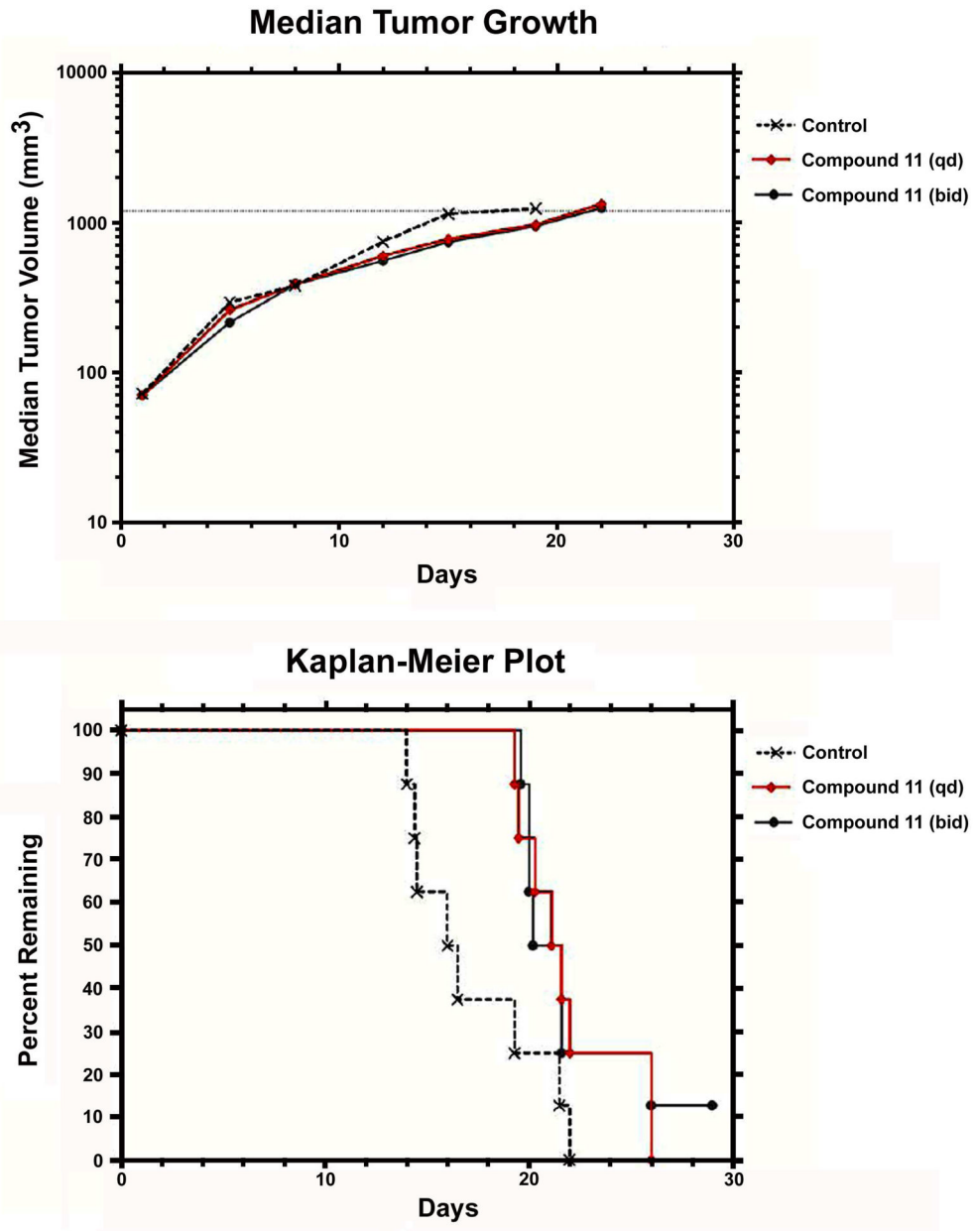

Figure 5.
In vivo antitumor activity of compound **11**

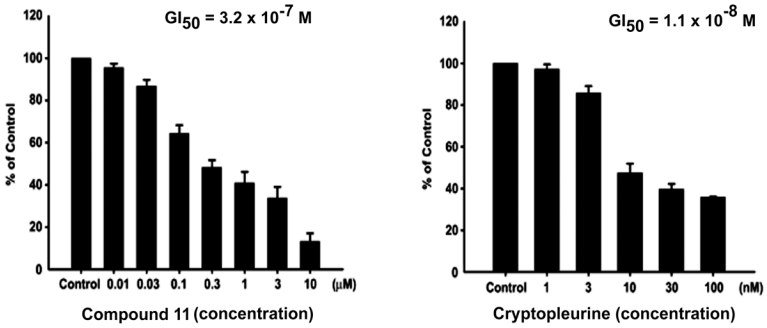

Figure 6.

Comparison of compound **11** and *R*-cryptopleurine against Human Umbilical Vein Endothelial Cells (HUVECs)

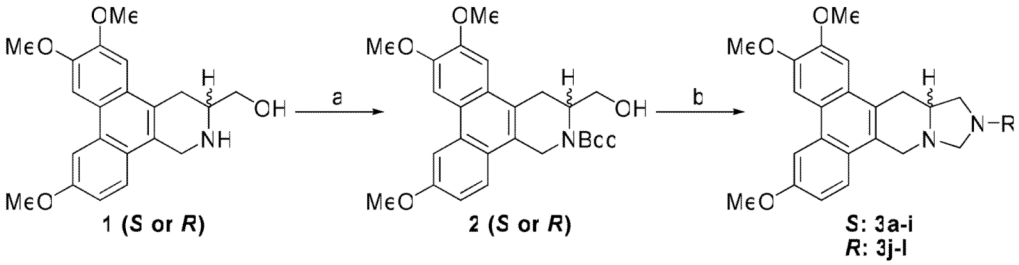

Scheme 1.

Reagents and conditions: (a) $(Boc)_2O$, Et_3N, CH_2Cl_2 (b) i) Py•SO_3, DMSO, Et_3N, CH_2Cl_2; ii) RNH_2, HOAc, $NaBH_3CN$, MeOH; iii) TFA, CH_2Cl_2; iv) K_2CO_3, $MgSO_4$, HCHO, CH_2Cl_2

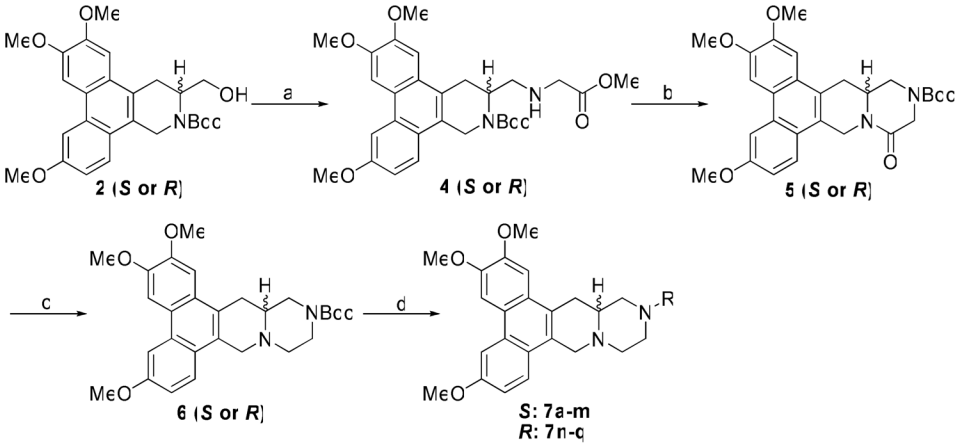

Scheme 2.

Reagents and conditions: (a) i) Py•SO_3, DMSO, Et_3N, CH_2Cl_2; ii) glycine methyl ester hydrochloride, Et_3N, HOAc, $NaBH_3CN$, MeOH (b) i) HCl, MeOH; ii) MeOH, Et_3N; iii) $(Boc)_2O$, Et_3N, CH_2Cl_2 (c) BMS, THF (d) i) TFA, CH_2Cl_2; ii) RCOCl, Et_3N, CH_2Cl_2 or RCHO, Et_3N, HOAc, $NaBH_3CN$, MeOH

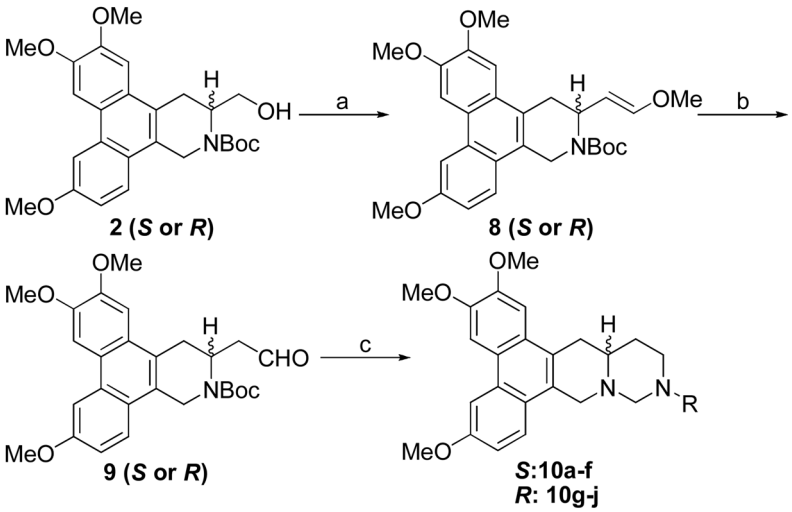

Scheme 3.

Reagents and conditions: (a) i) Py•SO_3, DMSO, Et_3N, CH_2Cl_2; ii) $Ph_3P^+CH_2OMeCl^-$, THF, KO*t*Bu (b) $Hg(OAc)_2$, THF, H_2O (c) i) RNH_2, HOAc, $NaBH_3CN$, MeOH; ii) TFA, CH_2Cl_2; iii) K_2CO_3, $MgSO_4$, HCHO, CH_2Cl_2

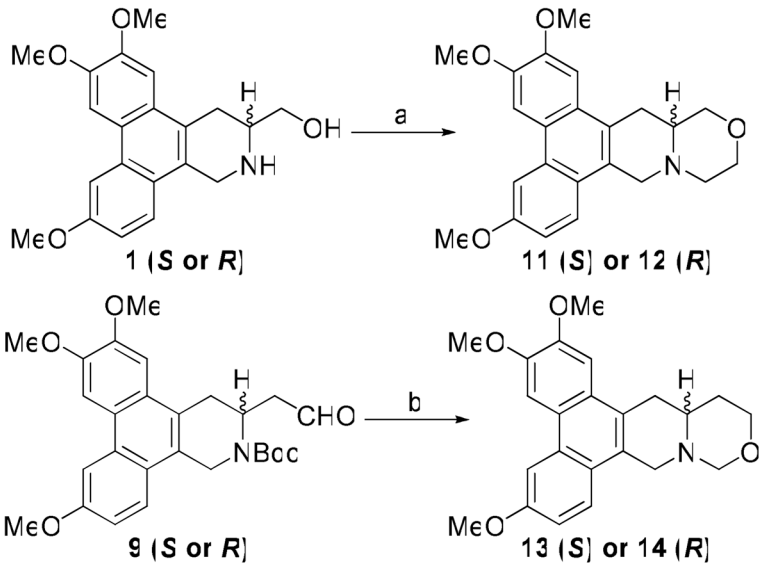

Scheme 4.

Reagents and conditions: (a) i) $ClCH_2COCl$, Et_3N, CH_2Cl_2; ii) NaH, THF, reflux; iii) BMS, THF (b) i) $NaBH_4$, MeOH; ii) TFA, CH_2Cl_2; iii) K_2CO_3, $MgSO_4$, HCHO, CH_2Cl_2

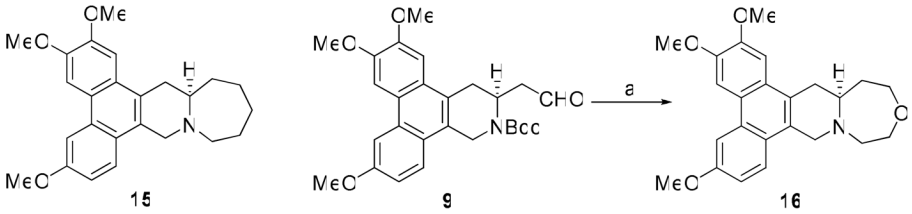

Scheme 5.

Reagents and conditions: (a) i) $NaBH_4$, MeOH; ii) TFA, CH_2Cl_2; iii) $ClCH_2COCl$, Et_3N, CH_2Cl_2, 0 °C; iv) NaH, THF, reflux; v) BMS, THF, 24% for 5 steps

Table 1

GI_{50} values of 12-aza-antofines **3a-l** against four cancer cell lines

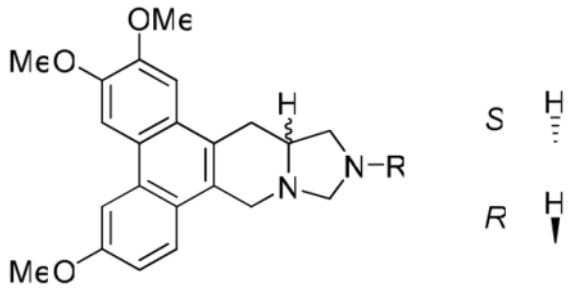

Compd.	R	Config.	A549 (μM)	DU145 (μM)	KB (μM)	HCT-8 (μM)
3a	-Bn	*S*	5.30 ± 1.02	4.95 ± 1.24	5.70 ± 1.52	3.63 ± 0.81
3b	-*i*Bu	*S*	2.00 ± 0.36	6.60 ± 1.45	4.40 ± 1.23	1.82 ± 0.45
3c	-*n*Pr	*S*	3.94 ± 0.78	7.38 ± 1.55	6.64 ± 1.73	2.71 ± 0.49
3d	$-(CH_2)_2Ph$	*S*	6.62 ± 2.04	10.20 ± 3.13	10.03 ± 2.11	7.47 ± 1.68
3e	-2′-OH-Et	*S*	4.41 ± 0.97	6.36 ± 1.29	7.83 ± 1.59	10.77 ± 2.44
3f	-Ph	*S*	> 20	> 20	> 20	> 20
3g	-*c*Pr	*S*	1.80 ± 0.36	3.70 ± 0.81	2.71 ± 0.89	1.85 ± 0.48
3h	-Me	*S*	0.66 ± 0.11	2.03 ± 0.38	1.72 ± 0.55	1.00 ± 0.19
3i	$-NMe_2$	*S*	1.67 ± 0.37	2.26 ± 0.47	2.31 ± 0.65	2.01 ± 0.54
3j	-Bn	*R*	2.68 ± 0.51	4.62 ± 1.16	3.41 ± 0.78	1.87 ± 0.43 (KBvin)
3k	$-NMe_2$	*R*	4.15 ± 0.87	6.01 ± 1.50	2.38 ± 0.60	10.98 ± 2.92 (KBvin)
3l	-Me	*R*	0.66 ± 0.10	1.00 ± 0.23	0.79 ± 0.21	0.66 ± 0.16
***R*-antofine**	-	*R*	22 ± 7 nM	25 ± 5 nM	36 ± 8 nM	-

Table 2

GI_{50} values of 13-aza-cryptopleurines **7a-q** against four cancer cell lines

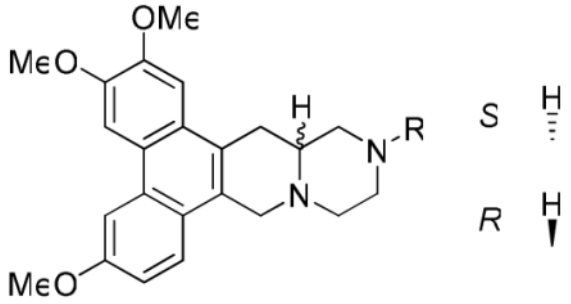

Compd.	R	Config.	A549 (μM)	DU145 (μM)	KB (μM)	HCT-8 (μM)
7a	H, HCl salt	*S*	1.73 ± 0.52	2.08 ± 0.27	1.79 ± 0.37	1.62 ± 0.56
7b	-Et	*S*	7.13 ± 3.86	10.48 ± 2.51	8.24 ± 1.89	9.45 ± 3.21
7c	$-CO_2Me$	*S*	10.93 ± 5.10	12.19 ± 3.04	11.32 ± 2.25	12.05 ± 2.58
7d	-Ac	*S*	11.65 ± 1.88	11.94 ± 2.22	15.46 ± 2.78	13.82 ± 2.80
7e	-Ms	*S*	14.52 ± 3.02	16.97 ± 3.14	17.52 ± 3.10	17.83 ± 3.63
7f	$-CH_2CO_2Me$	*S*	14.74 ± 2.49	> 20	14.65 ± 2.88	14.03 ± 2.12
7g	$-CH_2$*c*Pr	*S*	0.79 ± 0.11	2.94 ± 0.45	6.57 ± 1.56	0.25 ± 0.11
7h	-*c*Pr	*S*	> 20	17.92 ± 5.28	> 20	13.02 ± 3.03
7i	-Bz	*S*	15.00 ± 3.77	15.71 ± 4.32	> 20	18.11 ± 4.91
7j	-2′-OH-Et	*S*	14.08 ± 5.49	12.62 ± 5.61	8.62 ± 2.44	7.41 ± 1.30
7k	$-PO(OMe)_2$	*S*	12.18 ± 3.18	14.66 ± 4.59	8.09 ± 1.02	10.42 ± 2.21 (KBvin)
7l	-Me	*S*	9.73 ± 1.81	7.13 ± 1.05	5.30 ± 0.46	6.45 ± 1.03
7m	-Bn	*S*	> 20	> 20	16.85 ± 5.64	15.24 ± 3.35 (KBvin)
7n	$-CONMe_2$	*R*	14.08 ± 1.86	13.12 ± 1.98	12.32 ± 2.15	11.41 ± 2.10 (KBvin)
7o	-*i*Bu	*R*	12.86 ± 2.31	12.24 ± 4.04	11.25 ± 2.36	9.96 ± 1.89 (KBvin)
7p	-Bz	*R*	16.43 ± 6.08	11.87 ± 3.92	12.14 ± 2.91	7.64 ± 1.07 (KBvin)
7q	$-CH_2$*c*Pr	*R*	> 20	> 20	> 20	13.44 ± 2.42 (KBvin)
crypto-pleurine	-	*R*	1.38 ± 0.56 nM	1.59 ± 0.53 nM	1.51 ± 0.33 nM	1.09 ± 0.20 nM

Table 3

GI_{50} values of analogs **10a-j** against four cancer cell lines

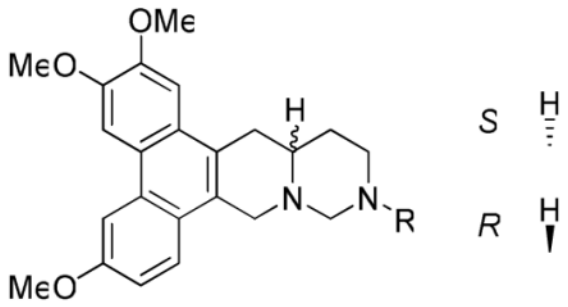

Compd.	R	Config.	A549 (μM)	DU145 (μM)	KB (μM)	HCT-8 (μM)
10a	-2′-OH-Et	*S*	5.68 ± 1.36	1.99 ± 0.52	1.59 ± 0.36	10.65 ± 3.73
10b	-Ph	*S*	> 20	> 20	> 20	> 20
10c	-*i*Bu	*S*	1.52 ± 0.38	2.30 ± 0.55	5.06 ± 1.82	1.36 ± 0.29
10d	-Bn	*S*	> 20	> 20	> 20	> 20
10e	-*c*Pr	*S*	4.30 ± 0.77	14.33 ± 3.80	11.47 ± 3.72	5.73 ± 1.14
10f	$-NMe_2$	*S*	1.78 ± 0.43	2.97 ± 0.51	3.08 ± 0.50	2.37 ± 0.78
10g	-*i*Bu	*R*	5.11 ± 1.62	1.66 ± 0.43	1.45 ± 0.22	7.32 ± 1.90 (KBvin)
10h	$-NMe_2$	*R*	5.20 ± 1.02	3.00 ± 0.65	2.84 ± 0.56	5.30 ± 1.18 (KBvin)
10i	-2′-OH-Et	*R*	2.48 ± 0.36	1.46 ± 0.33	2.22 ± 0.41	> 20 (KBvin)
10j	$-CH_2$*c*Pr	*R*	1.12 ± 0.29	1.20 ± 0.28	2.10 ± 0.39	5.68 ± 1.53 (KBvin)
crypto-pleurine	-	*R*	1.38 ± 0.56 nM	1.59 ± 0.53 nM	1.51 ± 0.33 nM	1.09 ± 0.20 nM

Table 4

GI_{50} values of analogs **11–14** against four cancer cell lines

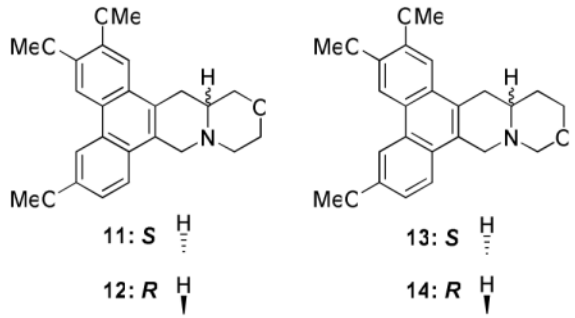

Compd.	Config.	A549	DU145	KB	HCT-8
11	*S*	23 ± 5 nM	67 ± 10 nM	37 ± 9 nM	9 ± 5 nM
12	*R*	13.95 ± 4.74 μM	7.05 ± 1.25 μM	6.68 ± 1.52 μM	3.45 ± 0.56 μM
13	*S*	1.79 ± 0.27 μM	1.82 ± 0.31 μM	1.66 ± 0.33 μM	1.45 ± 0.24 μM
14	*R*	1.37 ± 0.29 μM	1.29 ± 0.36 μM	1.10 ± 0.28 μM	1.26 ± 0.20 μM
crypto-pleurine	*R*	1.38 ± 0.56 nM	1.59 ± 0.53 nM	1.51 ± 0.33 nM	1.09 ± 0.20 nM

Table 5

GI_{50} values of compounds **15** and **16**

Compd.	Config.	A549 (nM)	DU145 (nM)	KB (nM)	HCT-8 (nM)
15	R	25 ± 5	179 ± 36	102 ± 19	10 ± 3
16	S	41 ± 9	119 ± 33	68 ± 10	20 ± 6